Lead Hydro Sodalite $[Pb_2(OH)(H_2O)_3]_2[Al_3Si_3O_{12}]_2$: Synthesis and Structure Determination by Combining X-ray Rietveld Refinement, ^1H MAS NMR FTIR and XANES Spectroscopy

Stefanie Eiden-Aßmann,[a]* A. M. Schneider,[b] Peter Behrens,[b] Michael Wiebcke,[a] Günter Engelhardt,[c] and Jürgen Felsche[a]

Abstract: Ion exchange of the sodium hydro sodalites $[Na_3(H_2O)_4]_2[Al_3Si_3O_{12}]_2$, $[Na_4(H_3O_2)]_2[Al_3Si_3O_{12}]_2$ and $[Na_4(OH)]_2[Al_3Si_3O_{12}]_2$ with aqueous $Pb(NO_3)_2$ solutions yielded, whichever reactant sodalite phase was used, the same lead hydro sodalite, $[Pb_2(OH)(H_2O)_3]_2[Al_3Si_3O_{12}]_2$. Thus, in the case of the non-basic reactant $[Na_3(H_2O)_4]_2[Al_3Si_3O_{12}]_2$ an overexchange occurs with respect to the number of non-framework cationic charges. Rietveld structure refinement of the lead hydro sodalite based on powder X-ray diffraction data (cubic, $a = 9.070$ Å, room temperature, space group $P\bar{4}3n$) revealed that the two lead cations within each polyhedral sodalite cage form an orientationally disordered dinuclear $[Pb_2(\mu\text{-}OH)(\mu\text{-}H_2O)(H_2O)_2]^{3+}$ complex. Due to additional lead framework oxygen bonds the coordination environment of each metal cation (CN 3+3) is approximately spherical, and clearly the lead 6s electron lone pair is stereochemically inactive. This is also suggested by the absence of a small peak at 13.025 keV, attributed in other $Pb^{2+}-O$ compounds to an electronic 2p – 6s transition, in the PbL_3 edge XANES spectrum. ^1H MAS NMR and FTIR spectra show that the hydrogen atoms of the aqua hydroxo complex (which could not be determined in the Rietveld analysis) are involved in hydrogen bonds of various strengths.

Keywords: host – guest chemistry · ion exchange · lead · sodalites · structure elucidation

Introduction

Sodalites are host – guest compounds based structurally on the space-filling arrangement of Federov $[4^6 6^8]$ truncated octahedra (known as β-cages in zeolite chemistry). Many compounds possessing this structural topology have been synthesized, with a vast number of chemical compositions. The host framework of 1:1 aluminosilicate sodalites consists of an alternating array of corner-sharing AlO_4 and SiO_4 tetrahedra; the cubic unit cell, with edges of approximately 9 Å, has the composition $[Al_3Si_3O_{12}]_2^{6-}$ and contains two β-cages. The negative framework charge is usually compensated by non-framework cations M^+; in addition, M^+A^- ion pairs and/or water molecules can be enclathrated, as expressed by the general formula $[M_{3+x}(A)_x(H_2O)_n]_2[Al_3Si_3O_{12}]_2$, where M and A denote singly charged cations and anions, respectively. Owing to their structural relationship to the well-known and industrially important zeolites A, X and Y, sodalites have been considered as model systems for investigating the various host – guest interactions, static statistical and/or dynamic guest disorder and structural phase transitions.[1] Sodalites have also attracted considerable attention for their intra-cage reaction chemistry and interesting materials properties (for example cathodochromism, photochromism or ion conduction) and as periodic host matrices for the spatial organization of quantum-sized semiconductor clusters and cluster arrays.[2] Quantum-size effects such as blue shifts in the optical absorption edges have been observed for aluminosilicate sodalites containing silver salts,[3] but may be due to strong electronic interactions between Ag^+ ions and the negatively charged framework rather than to the spatial organization of quantum-sized clusters within the crystalline host framework.[4]

The synthesis of zeolites containing electronically soft divalent metal cations by ion-exchange reactions has been reported, and Pb^{2+} ions have been shown to give high exchange rates.[5] Crystal structures of Pb^{2+}-ion-exchanged zeolite A and some of its partially and completely dehydrated forms were determined by single-crystal X-ray crystallography.[6] For the hydrated zeolite A species, various polynuclear

---

[a] Dr. S. Eiden-Aßmann, Dr. M. Wiebcke, Prof. Dr. J. Felsche
Universität Konstanz, Fakultät für Chemie
78434 Konstanz (Germany)
Fax: (+49) 7531-88-3898
E-mail: assmann@vg3.chemie.uni-konstanz.de

[b] A. M. Schneider, Prof. Dr. P. Behrens
Universität Hannover, Institut für Anorganische Chemie
30167 Hannover (Germany)

[c] Prof. Dr. G. Engelhardt
Universität Stuttgart, Institut für Technische Chemie I
70550 Stuttgart (Germany)

lead hydroxo complexes which are somewhat similar to lead complexes present in aqueous solutions have been discussed. Zeolite A samples into which PbI_2 had been inserted showed blue shifts in their UV/visible adsorption edges that depended on the degree of PbI_2 loading.[7]

As part of our investigations into the synthesis, structure and properties of aluminosilicate sodalites containing soft metal cations,[8, 9] we have studied the ion exchange of the three well-characterized sodium hydro sodalites, $[Na_3(H_2O)_4]_2[Al_3Si_3O_{12}]_2$, $[Na_4(H_3O_2)]_2[Al_3Si_3O_{12}]_2$, and $[Na_4(OH)]_2[Al_3Si_3O_{12}]_2$,[10, 11] with aqueous $Pb(NO_3)_2$ solutions. Whichever reactant sodium hydro sodalite phase we used, we obtained the same lead hydro sodalite, $[Pb_2(OH)(H_2O)_3]_2[Al_3Si_3O_{12}]_2$. Here we report primarily the characterization of this lead hydro sodalite by means of Rietveld structure refinement based on powder X-ray diffraction data and ^1H MAS NMR, FTIR, and XANES (X-ray adsorption near-edge structure) spectroscopy. Full details of the ion-exchange behavior will be presented elsewhere, along with the ion-exchange characteristics of other soft metal cations with sodium hydro sodalites.[12]

Experimental Section

Synthesis and methods of characterization: The three reactant sodium hydro sodalite phases were synthesized and ion-exchanged with aqueous 0.1M $Pb(NO_3)_2$ solutions at 110 °C for 24 h, as described elsewhere.[11] Cation-exchange rates were determined by flame photometry (Na content of the solutions after exchange) and X-ray fluorescence spectroscopy (Pb content of solid product). The water/hydroxide-ion content was determined on a Netzsch STA 429 thermoanalyser combining thermogravimetry (TG), differential thermogravimetry (DTG), and differential thermal analysis (DTA), with heating rates of $10\,K\,min^{-1}$ under flowing nitrogen.

Phase identity and purity were checked by powder X-ray photographs taken on a Guinier camera (Huber system G 600) with $Cu_{K\alpha_1}$ radiation. Scanning electron micrographs (SEMs) were obtained on a JEOL JSM-840A instrument.

^1H MAS NMR spectra were recorded on a Bruker MSL-400 spectrometer (resonance frequency 400.13 MHz; pulse repetition 5 s; pulse width 1 µs; spin speed 10.0 kHz). Mid-IR spectra were recorded on a Mattson–Polaris FTIR spectrometer with KBr pellets of the samples.

X-ray absorption spectroscopic measurements of lead hydro sodalite and the reference compounds were carried out at the SRS (Synchrotron Radiation Source, Daresbury, UK), station 9.3, which was equipped with a Ge(311) double monochromator. The PbL_3 edge XANES spectra were obtained in transmission mode under ring operation conditions (1.998 GeV, 230–140 mA). The data were analysed with the programs Analysis, Opera and Exfit, developed by Niemann.[13]

X-ray Rietveld analysis: The powder X-ray diffraction pattern of $[Pb_2(OH)(H_2O)_3]_2[Al_3Si_3O_{12}]_2$ was recorded at room temperature on a Huber G 642 diffractometer with $Cu_{K\alpha_1}$ radiation (Ge monochromator). The powdered material was held between two transparent foils (flat sample), and the sample holder was moved tangentially to the focal circle during the measurement. The diffraction pattern was measured in the range $4^\circ \leq 2\theta \leq 100^\circ$ with a step width of 0.02°(4800 data points).

The background of the pattern was subtracted manually, and a profile function was determined employing Bärlocher's Learned Peak Shape function[14] on the (310) reflection ($2\theta = 31.158^\circ$). The powder data were analysed with the XRS-82 program[15] using the Rietveld method. Atomic scattering factors were taken from ref.[16]. Results below $2\theta = 11.66^\circ$ were excluded from the Rietveld analysis since no reflections were detected in that region. Space group $P\bar{4}3n$ was consistent with the reflection conditions and was later confirmed by structure refinement. The starting coordinates for the least-squares refinement were those of the Si, Al, and O1 atoms of the framework structure according to ref. [17], where the structure of $[Na_4(CH_3COO)]_2[Al_3Si_3O_{12}]_2$ is described. The lattice constant of this compound is similar to that of lead hydro sodalite. After adjustment of some profile parameters (zero-point and peak-asymmetry corrections) and cautious relaxation of the coordination of the framework O1 atom, it was possible to determine the position of the Pb^{2+} ions. The position of the oxygen atoms of the hydroxyl group and water molecules could be determined in subsequent difference Fourier syntheses of the electron density.

The further refinement procedure included the relaxation of the profile parameters, positions and displacement parameters of all atoms. In the final cycles of refinement the lead cation was treated anisotropically, while the remaining atoms were refined with isotropic displacement parameters. A final difference Fourier synthesis revealed maximum electron density at the final position of Pb^{2+} ($\Delta\delta = 2.9\,e^{-1}\,Å^{-3}$). Further details of the X-ray measurements and Rietveld analysis are given in Table 1.

Table 1. Crystal data and details of the measurement of powder X-ray diffraction and Rietveld refinement for $[Pb_2(OH)(H_2O)_3]_2[Al_3Si_3O_{12}]_2$.[a]

powder X-ray data collection	Ge monocromator, $Cu_{K\alpha_1}$ radiation, $\lambda = 1.54051$ Å range of measurement: $11.66^\circ \leq 2\theta = 100^\circ$, 2θ step width 0.02°, 81 contributing reflections, 4417 observations (3993 data points used for refinement).
number of parameters refined	profile parameters: atomic parameters: 10
number of refined parameters in final cycle	17
R factors	$R_F = 0.075$, $R_I = 0.070$ $R_{wp} = 0.153$, $R_{exp} = 0.156$ $\chi^2 = 0.98$, $\Delta/\sigma < 0.016$
final difference Fourier synthesis	$\Delta\rho_{max} = +2.88\,e\,Å^{-3}$ (at 0.153, x, x)

[a] The thermal parameters of the lead cation were refined anisotropically (see Table 2).

Results

Synthesis: Treatment of each of the sodium hydro sodalites $[Na_3(H_2O)_4]_2[Al_3Si_3O_{12}]_2$, $[Na_4(H_3O_2)]_2[Al_3Si_3O_{12}]_2$, and $[Na_4(OH)]_2[Al_3Si_3O_{12}]_2$ with aqueous 0.1M $Pb(NO_3)_2$ solution at 110 °C readily affords complete exchange of all nonframework sodium cations with divalent lead cations with retention of the sodalite host structure. Moreover, whichever reactant sodium sodalite is used, the same lead hydro sodalite is obtained.

Our combination of analytical techniques suggests the idealized chemical composition $[Pb_2(OH)(H_2O)_3]_2[Al_3Si_3O_{12}]_2$ for the product phase. X-ray powder photographs showed that the crystallinity of the reactant sodalites is essentially preserved during ion exchange and that the product is a pure-phase material, if optimized reaction conditions are used.[12] No amorphous by-products were visible on scanning electron micrographs, so all analytical data refer to the crystalline compound. The approximate ion-exchange rates determined experimentally were 120 % for $[Na_3(H_2O)_4]_2[Al_3Si_3O_{12}]_2$, 95 % for $[Na_4(H_3O_2)]_2[Al_3Si_3O_{12}]_2$ and 90 % for $[Na_4(OH)]_2[Al_3Si_3O_{12}]_2$. Simultaneous thermal analysis curves of the product phase are shown in Figure 1. The total mass loss of 7.39 % observed in the range 120–550 °C corresponds to the release of seven water molecules

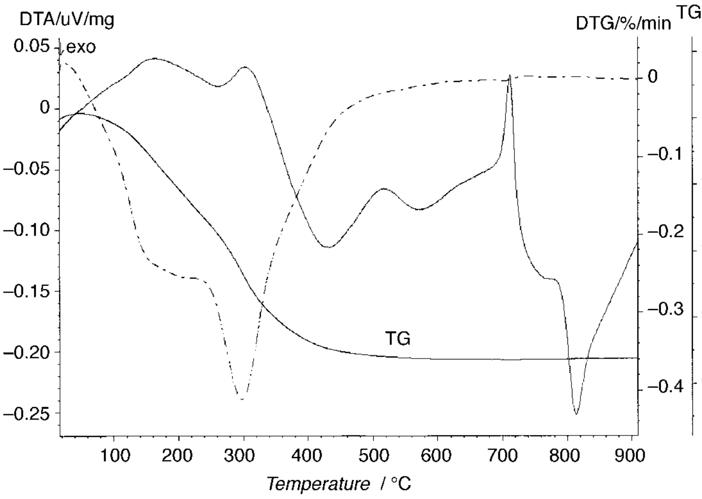

Figure 1. Simultaneous thermal analysis (TG/DTG/DTA) of lead hydro sodalite $[Pb_2(OH)(H_2O)_3]_2[Al_3Si_3O_{12}]_2$. –·– DTG, —— DTA.

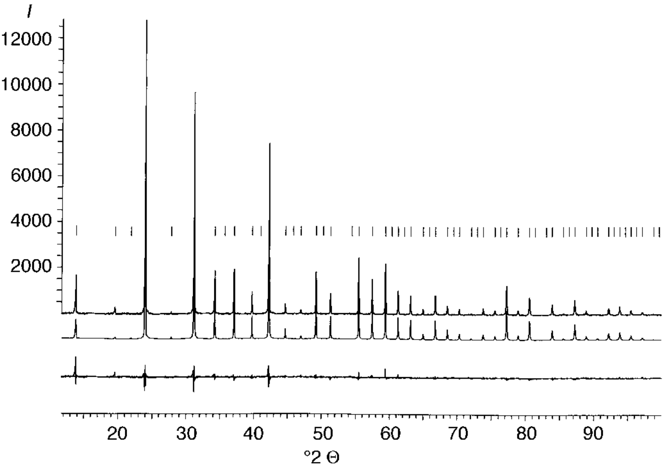

Figure 2. Observed (I_{obs}), calculated (I_{calc}) and difference ($I_{diff} = I_{obs} - I_{calc}$) powder diffraction pattern of $[Pb_2(OH)(H_2O)_3]_2[Al_3Si_3O_{12}]_2$. I = intensity [counts].

per formula unit (theoretical value: 7.48 %), with one of these stemming from two hydroxide ions.

The composition $[Pb_2(OH)(H_2O)_3]_2[Al_3Si_3O_{12}]_2$ implies that an overexchange occurs in the case of the reactant $[Na_3(H_2O)_4]_2[Al_3Si_3O_{12}]_2$: that is, more lead cations enter the sodalite structure than are needed to compensate for the six negative framework charges per formula unit. This is accompanied by simultaneous uptake of the appropriate number of hydroxide ions.

Table 2. Fractional atomic coordinates, thermal parameters U and statistical population parameter (PP) for $[Pb_2(OH)(H_2O)_3]_2[Al_3Si_3O_{12}]_2$ (see Table 1).

Atom	Wyckoff position	x	y	z	U_{11}	U_{12}	PP
Si	6c	1/4	1/2	0	0.009(2)[a]	0	1.0
Al	6d	1/4	0	1/2	0.009[a]	0	1.0
O1	24i	0.1442(7)	0.1525(7)	0.4547(7)	0.031(3)	0	1.0
Pb	8e	0.1515(1)	0.1515	0.1515	0.0172(5)[c]	0.0104(8)[a]	0.5[b]
O2	8e	0.3991(6)	0.3991	0.3991	0.089(6)	0	1.0

[a] U(Si) and U(Al) were refined as coupled parameters, U(Al) = U(Si). [b] PP(Pb) was fixed during the refinement procedure. [c] U(11) = U(22) = U(33) and U(12) = U(13) = U(23).

X-ray Rietveld analysis: At room temperature $[Pb_2(OH)(H_2O)_3]_2[Al_3Si_3O_{12}]_2$ is cubic ($a = 9.070$ Å; space group $P\bar{4}3n$). The experimental and simulated X-ray diffraction profiles are displayed in Figure 2. Structural data are summarized in Tables 2 and 3. The interatomic distances and angles of the sodalite host framework, with strict alternation of corner-sharing AlO_4 and SiO_4 tetrahedra, are in the expected ranges.

Lead cations and oxygen atoms of water molecules and hydroxide ions are found at Wyckoff positions 8e on the body diagonal of the unit cell. They constitute a larger Pb and a smaller O2 tetrahedron (together forming a distorted cube) around each cage center (Figure 3a). The Pb site has a statistical population parameter of 0.5 according to the thermogravimetric results, while the O2 site with a population parameter of 1.0 is fully occupied by oxygen atoms from both water and hydroxide. Each lead cation is bonded to three equidistant guest O2 atoms (d(Pb−O2) = 2.380(6) Å) and three equidistant framework O1 atoms (d(Pb−O1) = 2.760(6) Å), resulting in (3+3) coordination (Figures 4 and 3c), which deviates considerably from an octahedral configuration. The structural analysis did not indicate any ordering of Pb^{2+} cations in adjacent cages. The shortest distance between the two lead cations is 3.886(1) Å.

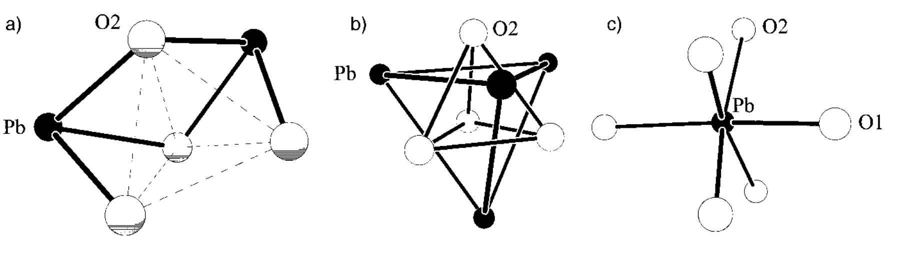

Figure 3. a) A large Pb and a small O2 tetrahedron (together forming a distorted cube) around each cage center. b) The cage contents of $[Pb_2(OH)(H_2O)_3]_2[Al_3Si_3O_{12}]_2$. c) The oxygen coordination of the lead cation.

Table 3. Selected interatomic distances [Å] and angles [°] for $[Pb_2(OH)(H_2O)_3]_2[Al_3Si_3O_{12}]_2$.

		Host structure		Lead		Coordination	
Al−O1	1.733(6)	Si−O1	1.631(6)	Pb1−O1	2.751(6)	O1-Pb-O1	91.2 (4)
O1-Al-O1 (4 ×)	107.9(3)	O1-Si-O1 (4 ×)	107.1(3)	Pb1-O1	3.127(6)	O1-Pb-O2	101.0 (4)
O1-Al-O1 (2 ×)	112.8(3)	O1-Si-O1 (2 ×)	114.4(3)	Pb1-Pb1	3.886(1)	O2-Pb-O2	65.9 (4)
Al-O1-Si	144.8(4)			Pb1−O2	2.380(6)		

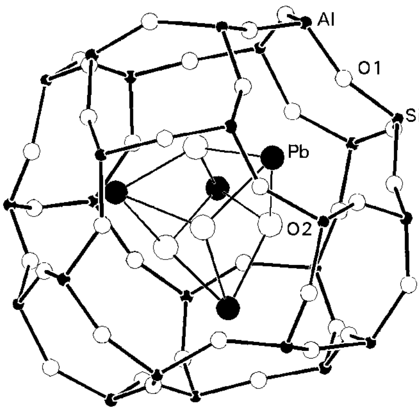

Figure 4. The results of the Rietveld refinement.

It was not possible to determine the position of hydrogen atoms in the Rietveld refinement. However, structural chemical arguments suggest a dinuclear $[Pb_2(\mu\text{-}OH)(\mu\text{-}H_2O)(H_2O)_2]^{3+}$ complex formulation with OH^- and H_2O bridging ligands and one terminal H_2O ligand at each Pb center (Figure 3b). This guest complex is sixfold orientationally disordered, each orientation corresponding to one of the six edges of the Pb tetrahedron. The Pb–O2 distance represents the space- and (possibly) time-average of three different bond types: one μ-HO–Pb, one μ-H_2O–Pb and one H_2O–Pb bond. These intra-complex Pb–O2 bonds are significantly shorter than the six Pb–O1 bonds to the host framework.

As a result of the disorder, the displacement parameter of the O2 atom is comparatively large, corresponding to a root-mean-square amplitude of 0.30 Å. The O2 ··· O2 (2.588(8) Å) and O1 ··· O2 (3.256(8) Å) distances each represent the average of different bonds, and allow, on the basis of geometrical criteria, the existence of different hydrogen bonds bridging guest oxygen atoms as well as linking guest oxygen atoms with those of the host framework. Information on the bonding of the hydrogen atoms has been obtained from the ^{1}H NMR and FTIR spectra reported below.

^{1}H MAS NMR and FTIR spectroscopy: The three broad, strongly overlapping signals in the room-temperature ^{1}H MAS NMR spectrum (Figure 5) can be reasonably well simulated with four component Gaussian lines, L1–L4, with chemical shifts of $\delta = 2.56$ (L1), 3.78 (L2), 5.30 (L3), and 7.00 (L4). The considerable linewidth of all the signals suggests that the protons possess only a limited degree of mobility on the NMR time scale at room temperature, so that the strong dipolar H–H interactions were not averaged effectively by the MAS technique employed. The chemical shifts reveal that the hydrogen atoms of the guest complex are involved in various hydrogen bonds of low to medium strength. Donor–acceptor O–O distances estimated from the δ values are between 2.82 and 3.00 Å, if an empirical linear correlation between proton chemical shifts and O–H ··· O distances given by Yesinowski et al.[18] is applied. These estimates have to be compared with the O2 ··· O2 and O1 ··· O2 distances in the disordered complex determined by the Rietveld analysis (2.588(8) and 3.256(8) Å), which are assumed to be based on a space- and (possibly) time-averaged picture of the disordered structure.

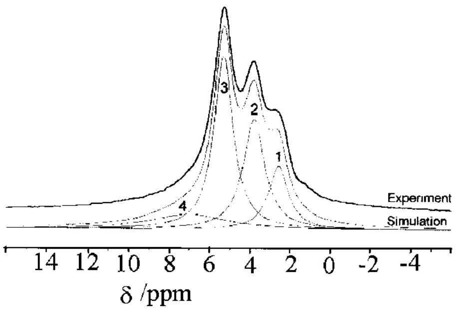

Figure 5. ^{1}H MAS NMR spectrum of the lead hydro sodalite.

Table 4. Results of the simulation of the ^{1}H NMR spectrum.

Gaussian line	δ [ppm]	rel. int. [%]	Assignment
L1	2.56	15	H1
L2	3.78	30	H2
L3	5.30	42	H3
L4	7.00	13	H4

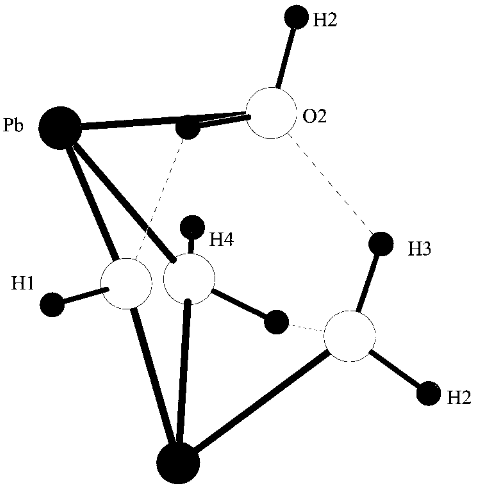

Figure 6. Approximate positions of the hydrogen atoms and a possible hydrogen bonding system for one orientation of the guest complex.

Chemical shifts, relative intensities and a tentative assignment of the signals to the protons of the $[Pb_2(\mu\text{-}OH)(\mu\text{-}H_2O)(H_2O)_2]^{3+}$ complex are summarized in Table 4. Corresponding approximate positions of the hydrogen atoms and a possible hydrogen bonding system are shown for one orientation of the guest complex in Figure 6. In this model, one hydrogen atom of each ligand is located on (or near) the body diagonal of the unit cell, and the covalent O–H bonds point to (or nearly to) the midpoints of six-membered rings of the aluminosilicate framework. Each of these hydrogen atoms participates in hydrogen bonds to three framework O1 atoms (three-center bonds). We assign these hydrogen atoms (one H1, two H2, one H4) according to the probable donor strength of the ligands (μ-OH < H_2O < μ-H_2O) to the signals L1, L2, and L4, following the order of increasing δ. The remaining hydrogen atoms of the water molecules (three H3), which we assign to the L3 signal, may be located near the edges of the

O2 tetrahedron and form a (dynamic) system of intracomplex hydrogen bonds, in which the μ-OH and μ-H_2O ligands act only as an acceptor and a donor, respectively.

In the room-temperature FTIR spectrum (Figure 7) the bands with wavenumbers above 3000 cm^{-1} (ν(OH)) indicate hydrogen bonds of low to medium strength, in accord with the ^{1}H NMR spectrum. The sharp bands at 3580 and 3520 cm^{-1} may be assigned to O2–H1 and O2–H2 stretching vibrations, respectively, corresponding to the weakest hydrogen bonds from the weakest donor, and the broad feature at lower wavenumbers (3000–3400 cm^{-1}) probably originates from O–H3 and O–H4 stretching vibrations. The H_2O deformation mode ($\delta(H_2O)$) is at 1650 cm^{-1}. The assignment of the feature at 1450 cm^{-1} is not so clearcut; it may be attributed to an (O–H···O) bending mode perturbed by hydrogen bonds.[19, 20] The bands below 1200 cm^{-1} are framework vibrations typical of aluminosilicate sodalites.[21]

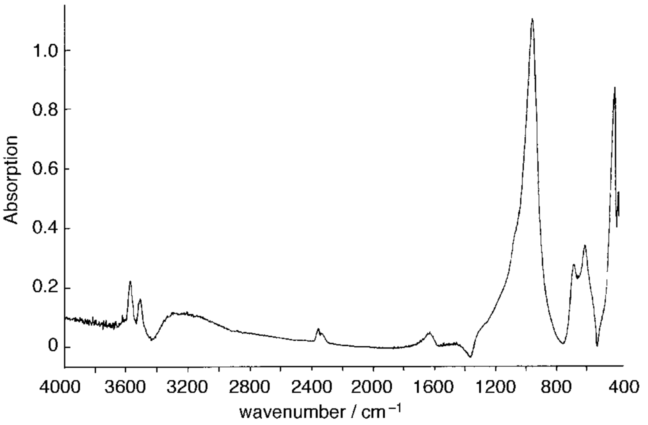

Figure 7. IR spectrum of lead hydro sodalite.

XANES spectroscopy: A high-intensity peak in the spectrum of PbO_2 at 13.025 keV (Figure 8) is attributed to a dipole-allowed electronic transition from a filled 2p orbital of the Pb^{4+} ion to the empty 6s orbital. In divalent lead compounds such a transition should not be observed, if the 6s orbital of the Pb^{2+} ion is assumed to be completely filled. Such a situation evidently exists in $[Pb_2(OH)(H_2O)_3]_2[Al_3Si_3O_{12}]_2$ and in $Pb(NO_3)_2$, since the spectrum of neither compound shows any feature at 13.025 keV. In contrast, in the spectra of Ag_2PbO_2 and β-PbO, a low-intensity peak is clearly visible at that energy (Figure 8).

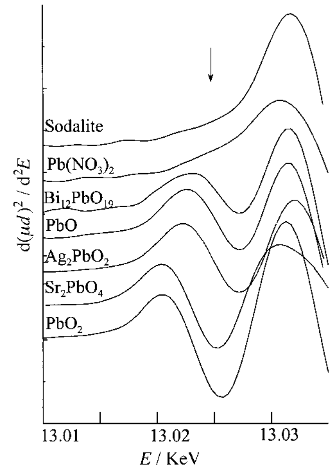

Figure 8. The second derivative of the PbL_3 edge XANES spectrum of lead hydro sodalite, with the second derivatives of the spectra of some lead–oxygen compounds, taken as references for lead in different valence states and coordination environments.

Comparison of the Pb^{2+} coordination environments reveals that in lead hydro sodalite and lead nitrate[22] the cations are surrounded, approximately spherically, by six oxygen atoms (although the coordination polyhedron deviates considerably from an ideal octahedron in the sodalite, as shown above). Apparently there is no free space at the lead cations that could be ascribed to the presence of a stereochemically active 6s electron pair; that is, the electron pairs are stereochemically inactive in both compounds. The situation is different for the other Pb^{2+}–O compounds (Ag_2PbO_2,[23] β-PbO[24]), where an open coordination of the lead cations points to a stereochemically active 6s lone pair. The stereochemical activity of this pair corresponds to a hybridization of the spherical s and directional p orbitals accompanied by a partial deoccupation of the 6s states. This explains why there is a small peak at 13.025 keV, which we attribute to a 2p–6s transition, in the PbL_3 XANES spectra of these compounds.

Discussion

Lead cations are readily ion-exchanged not only into aluminosilicate zeolites, as reported in the literature,[5] but also into aluminosilicate sodalites that contain only very small six-membered rings, the free aperture of which (approximately 2.6 Å) only slightly exceeds the diameter of the unsolvated Pb^{2+} ion (2.4 Å). The ease of ion exchange by the lead cation results from a favorable combination of its physicochemical properties, namely high polarizability, low hydration number and high charge.[25] Pb^{2+} is the only cation known so far to give an overexchange with simultaneous uptake of hydroxide ions for $[Na_3(H_2O)_4]_2[Al_3Si_3O_{12}]_2$. Using this reactant in the ion exchange of other cations (Cd^{2+}, Zn^{2+}, Cu^{2+}, Ag^+) we have obtained only hydroxide-free hydro sodalites.[8] NaOH is readily extracted from the basic hydro sodalite $[Na_4(H_3O_2)]_2[Al_3Si_3O_{12}]_2$ by treatment with water; indeed, this is the only known method of obtaining non-basic $[Na_3(H_2O)_4]_2[Al_3Si_3O_{12}]_2$.[26] The reverse reaction has not been reported. Aqueous solutions of Pb^{2+} salts, for example $Pb(NO_3)_2$, are known to contain various cationic lead hydroxo complexes due to hydrolysis;[27] the hydrolysed mononuclear species $[Pb(OH)]^+$ may be a vehicle of hydroxide migration into the sodalite structure.

The Pb–O and Pb···Pb distances found for the disordered $[Pb_2(\mu\text{-}OH)(\mu\text{-}H_2O)_2(H_2O)_2]^{3+}$ complex of lead hydro sodalite agree with those reported in the literature for oligonuclear lead hydroxo complexes in some crystalline salt hydrates.[28] The Pb···Pb distance is 0.39 Å longer than in metallic lead. Such long distances in lead compounds are usually taken to indicate that metal–metal attractive interactions are not relevant.[29] In comparison, the short Ag–Ag distances in

$[Ag_3(H_2O)_4]_2[Al_3Si_3O_{12}]_2$ are probably caused by weak $d^{10}-d^{10}$ attractive interactions which stabilize the disordered trinuclear silver–aqua cluster in this hydro sodalite.[30]

Various lead hydroxo complexes have been found, by single-crystal X-ray structural studies, as guest species in the β- and α-cages of overexchanged lead zeolite A. A trinuclear $[Pb_3(\mu_3\text{-}O)(\mu_3\text{-}OH)_3]^+$ and a dinuclear $[Pb_2(\mu_3\text{-}OH)]^{3+}$ unit, respectively, both disordered and bonded via oxygen atoms through the six-membered tetrahedral rings to further lead cations located in adjacent large α-cages, are present in the sodalite cages of zeolite A. In their general bonding geometries, these species are similar to the $[Pb_2(\mu\text{-}OH)(\mu\text{-}H_2O)(H_2O)_2]^{3+}$ complex in lead hydro sodalite. The lead cations within each sodalite cage are bonded to three framework oxygen atoms. The compositons of the complexes differ, however, and inter-complex bonds, extending through the six-membered rings between adjacent cages, do not exist in lead hydro sodalite (the shortest inter-complex Pb $\cdots$ O distance is 3.888 Å).

The interpretation of the peak at 13.025 keV in the XANES spectra of some Pb^{2+} compounds contrasts with that of Yu et al.,[31] who assigned it to a 2s–6d transition. In that case the intensity of the peak should be independent of the coordination of the lead cation, which is not observed.Thus, XANES spectroscopy provides a tool for differentiating between open and spherical coordination environments of Pb^{2+} ions—that is, between 6s lone pairs that are stereochemically active and inactive, respectively. This should be of particular interest for amorphous and finely grained crystalline materials that cannot be prepared as single crystals suitable for X-ray structural analysis.

Acknowledgements

Help from the staff at Daresbury Laboratory, especially R. Bilsborrow, is gratefully acknowledged. These measurements were supported by the European Large Scale Facilities Programme. The work was furthermore supported by the Fonds der Chemischen Industrie and the Deutsche Forschungsgemeinschaft (DFG).

[1] J. Felsche, S. Luger, *Thermochim. Acta* **1987**, *118*, 35.
[2] G. A. Ozin, A, Kupermann, A. Stein, *Angew. Chem.* **1989**, *101*, 373; *Angew. Chem. Int. Ed. Engl.* **1989**, *28*, 359.
[3] A. Stein, G. A. Ozin, G. D. Stucky, *J. Am. Chem. Soc.* **1992**, *114*, 8119.
[4] P. Behrens, *Solid State Commun.* **1992**, *81*, 325.
[5] E. Hertzenberg, H. Sherry, *ACS Symp. Ser.* **1980**, *135*, 187.
[6] C. Ronay, K. Seff, *J. Phys. Chem.* **1985**, *39*, 1965.
[7] O. Terasaki, Z. K. Tang, Y. Nozue, T. Goto, *Mater. Res. Soc. Symp. Proc.*, **1991**, *233*, 139.
[8] S. Aßmann, Dissertation, Konstanz, **1994**; Hartung–Gorre-Verlag Konstanz, ISBN 3-89191-793-7.
[9] P. Behrens, B. P. Kempa, S. Aßmann, M. Wiebcke, J. Felsche, *J. Solid State Chem.* **1995**, *114*, 1639.
[10] J. Felsche, S. Luger, P. Fischer, *Acta Crystallogr. Sect. C* **1987**, *43*, 809.
[11] M. Wiebcke, G. Engelhardt, J. Felsche, P. B. Kempa , P. Sieger, J. Schefer, P. Fischer, *J. Phys. Chem.* **1992**, *96*, 392.
[12] S. Eiden-Aßmann, unpublished results.
[13] W. Niemann, unpublished X-ray analysis results YXLON-International X-ray, Hamburg.
[14] A. Hepp, C. Baerlocher, *Aust. J. Phys.* **1988**, *42*, 229.
[15] C. Bärlocher, *The X-ray Rietveld System*, ETH Zürich, **1998**.
[16] *International Tables of X-ray Crystallography*, *Vol. IV*, Kynoch Press, Birmingham, **1974**, pp. 99, 149.
[17] P. Sieger, A. M. Schneider, M. Wiebcke, P. Behrens, J. Felsche, G. Engelhardt, *Chem. Mater.* **1995**, *7*, 163.
[18] J. P. Yesinowski, H. Eckert, G. R. Rossmann, *J. Am. Chem. Soc.* **1988**, *110*, 1367.
[19] L. Smith, A. K. Cheetham, R. E. Morris, L. Marchese, J. M. Thomas, P. A. Wright, J. Chen, *Science* **1996**, *271*, 799.
[20] J. Sauer, P. Legliengo, E. Garroue, V. R. Saunders, *Chem. Rev.* **1994**, *94*, 2095.
[21] C. M. B. Henderson, D. Taylor, *Spectrochim. Acta Part A* **1979**, *35*, 929.
[22] H. Nowotny, G. Heger, *Acta Crystallogr. Sect.* C **1986**, *42*, 133.
[23] A. Bystroem, L. Evers, *Acta Chem. Scand.* **1988**, *42*, 613.
[24] P. Boher, P. Garnier, J. R. Gavarri, A. W. Hewat, *J. Solid State Chem.* **1985**, *57*, 343.
[25] H. E. Allen, S. H. Cho, T. A. Neubecker, *Water Res.* **1983**, *17*, 1871.
[26] G. Engelhardt, J. Felsche, P. Sieger, *J. Am. Chem. Soc.* **1992**, *114*, 1173.
[27] C. F. Baes, R. E. Mesmer, *Hydrolysis of Cations*, Wiley, New York, **1976**, Chapter 15.
[28] G. Johansson, A. Olin, *Acta Chem. Scand.* **1990**, *84*, 351.
[29] G. Johansson, A. Olin, *Acta Chem. Scand.* **1968**, *24*, 3091.
[30] S. Eiden-Aßmann, A. M. Schneider, unpublished results.
[31] Y. U. Yu, T. Tyliszczak, A. D. Hitchcock, *Phys. Chem. Solids* **1990**, *51*, 445.

Received: March 26, 1999 [F 1699]